ФЕДЕРАЛЬНОЕ ГОСУДАРСТВЕННОЕ БЮДЖЕТНОЕ УЧРЕЖДЕНИЕ НАУКИ
ИНСТИТУТ КОСМИЧЕСКИХ ИССЛЕДОВАНИЙ
РОССИЙСКОЙ АКАДЕМИИ НАУК

ИКИ
ИНСТИТУТ
КОСМИЧЕСКИХ
ИССЛЕДОВАНИЙ
РАН

МЕЖДУНАРОДНАЯ КОНФЕРЕНЦИЯ
INTERNATIONAL CONFERENCE

ВЛИЯНИЕ КОСМИЧЕСКОЙ ПОГОДЫ НА ЧЕЛОВЕКА В КОСМОСЕ И НА ЗЕМЛЕ

4–8 ИЮНЯ/JUNE 2012

SPACE WEATHER EFFECTS ON HUMANS IN SPACE AND ON EARTH

ИНСТИТУТ КОСМИЧЕСКИХ ИССЛЕДОВАНИЙ
SPACE RESEARCH INSTITUTE

ТРУДЫ МЕЖДУНАРОДНОЙ КОНФЕРЕНЦИИ

1

Под редакцией

вице-президента РАН
академика
А. И. Григорьева
и академика РАН
Л. М. Зелёного

В двух томах

МОСКВА
2013

AN ANALYSIS OF THE HIGH-SPEED SOLAR WIND STREAMS ACTIVITY DURING SOLAR CYCLE 23: SOURCES OF RADIATION HAZARDS IN GEOSPACE

G. Xystouris, E. Sigala, H. Mavromichalaki

Nuclear and Particle Physics Section, Physics Department, National
and Kapodistrian University of Athens, Zografos 15784 Athens Greece,
e-mail: emavromi@phys.uoa.gr; xystouris_geo@hotmail.com; e.s.asteraki@hotmail.com

The High Speed Solar Wind Streams (HSSWSs) are ejected from the Sun and travel into the interplanetary space. Due to their high speed, they carry out energetic particles, such as protons and heavy ions that result to the increment of the mean interplanetary magnetic field. While the Earth is in the path of those HSSWSs, Earth's magnetosphere interacts with the disturbed magnetic field, leading to significant radiation-induced degradation of technological systems, provide an enhanced energy transfer from the solar wind/IMF system into the Earth magnetosphere and initiate geomagnetic disturbances having a possible impact on human health. The 23rd solar cycle was particularly unusual, with many energetic phenomena occurred during its descending phase and the existence of an extended minimum. In this study, we have identified and catalogued the HSSWSs for the 23rd solar cycle. We determined many characteristics of the streams, such as their maximum velocity, their beginning and ending time, their duration, their possible sources etc. Also, we studied the distributions through the solar cycle for many of their parameters. We regard that this catalogue would be helpful for the monitoring of Space Weather and possible predictions for it, the study of possible influence of Space Weather on human health, the planning of future space missions etc.

INTRODUCTION

One of the most important solar terrestrial phenomena is undeniable the near-Earth solar wind flow. It is known that the flow of solar wind is connected with a wide range of phenomena and effects, that become perceptible not only in space, but also on Earth, e.g. the space weather, the reduction of the distance of magnetopause, the geomagnetic storms, the aurora, the solar radiation storms, the radio blackouts. The solar wind flow is a continuous flow, with an average speed of 250...400 km·s^{-1} [Parker, 1959] and it tends to be organized on stream structure [Iucci et al., 1979]. When a stream is generated with a flow speed over 400 km·s^{-1}, its velocity is greater than the local velocity of solar wind. Hence, a tangential discontinuity to the solar wind flow is created and a shock wave occurs. In that way high-speed solar-wind streams (HSSWSs) are created.

Through the years there have been many definitions for the High Speed Solar Wind Stream (HSSWS). According to [Bame et al., 1976; Gosling et al., 1976], a HSSWS is an observed variation of solar wind speed, with an increase of at least 150 km·s^{-1} within a 5-day interval [Intrilligator, 1977] described it as a rapidly increase of the solar wind stream with a peak speed equal or greater than 450 km·s^{-1}. Also, [Broussard et al., 1978] described it as a period in which the solar wind speed is equal or greater than 500 km·s^{-1}, averaged over a day. Later, [Lindblad, Lundstedt, 1981] defined it as a period in which the velocity difference between the smallest 3-hour velocity value and the largest 3-hour value of the following day is equal or greater than 100 km·s^{-1} and it lasts for at least two days. Finally, according to [Mavromichalaki et al., 1988, 1997] a HSSWS is defined as the difference between the maximum speed and the mean plasma speed between the mean speed immediately preceding and following the stream is equal or greater than 100 km·s^{-1}, in a period lasting for at least two days.

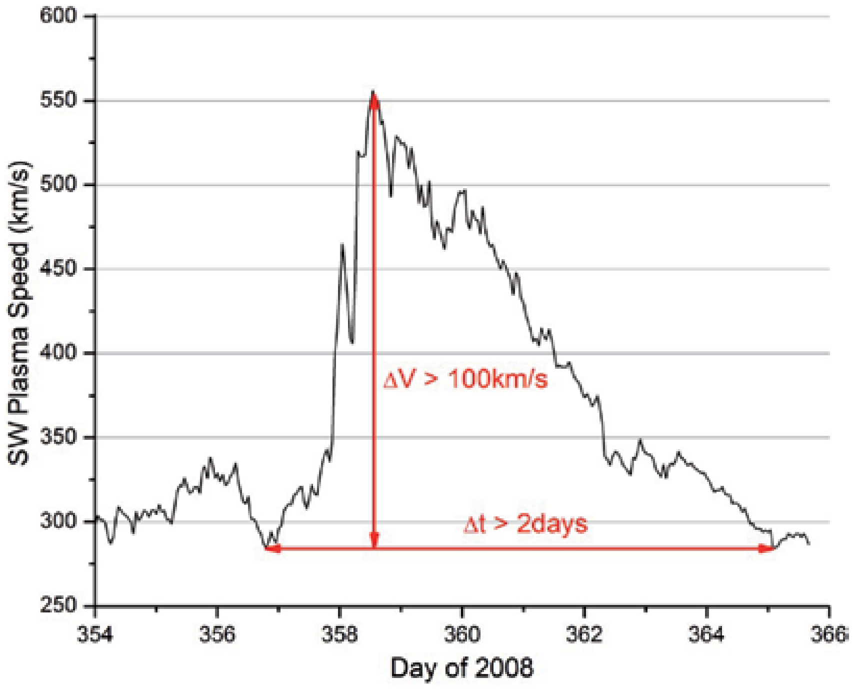

Figure 1. A typical example of a HSSWS. The speed difference is over 100 km·s^{-1}, while the period of the solar wind coming back to its initial speed is over two days

This definition is used in this work because it is more adequate for solar-terrestrial studies and it is in agreement with our previous studies. A typical example of a HSSWS is shown in Figure 1.

The HSSWSs are produced either by corotating coronal holes or by solar flare activity. A corotating coronal hole is a low temperature and low density area on the Sun's surface. As the Sun rotates, coronal holes pass across the Sun-Earth line and as the HSSWS are emitted from the Sun, they catch up with the previously emitted solar wind. In that way, they form a compressed interface in the interplanetary medium called a corotating interaction region [Morley et al., 2009]. The physical features of the corotating streams, according to [Mavromichalaki and Vassilaki, 1998] are the following:

- the interplanetary magnetic field (B) magnitude is proportional to bulk speed and the polarity is constant throughout the speed except for some fluctuations lasting a few hours;
- the proton density (n) rises to unusually high values near the leading edges of the streams vice to bulk speed;
- the proton temperature (T) varies with the same way as the flow speed.

Until recently, the HSSWSs that come from a blast wave were connected only with the flares activity. Nowadays, due to the development of technology for the solar observations, HSSWSs can be connected not only with flares, but also with coronal mass ejections (CMEs). In that process the material ejected by the flares, because of its expansion, compresses the plasma of the slower moving solar wind ahead the stream and the field lines, causing, at the leading edge of the slower moving surrounding plasma, a segregation surface with different thermodynamical and chemical properties in each side [Hollweg, 1974]. This structure is prevented from breaking apart due to its high electrical conductivity. At the point that the emitted solar wind plasma obtains a velocity greater than the local Alfvén velocity, the shock wave is created. Finally, as the previous situation of the coronal hole, a HSSWS is created. The behaviours of interplanetary parameters of the flare-generated streams tend to be irregular. In a general way we can admit that:

- all the interplanetary parameters show simultaneous increases. Especially, the bulk speed (V), the proton density (n) and the magnetic field magnitude (B) show large fluctuations during the period of the maximum speed value. Probably this indicates radially outcoming fast shocks;
- during the maximum speed period, the field polarity shows inversions lasting for 3...4 hours.
- the proton temperature does not vary simultaneously to the flow speed, but it tends to divert from speed behaviour, on contrary to corotating streams.

The reason for studying HSSWSs is because they are a potential hazard for the Earth. They contain very energetic particles, which are the source of the solar radiation. We can divide the dangerous areas into the Geospace and the Earth atmosphere and ground. The hazards for the Geospace regard hazards for the satellites — the technological instruments in general — and the astronauts. The hazards for Earth atmosphere and its ground contain regard for the technological instruments but also for humans. The greatest danger for humans is for the aircraft passengers, due to the thinner atmospheric layer above them (for blocking the energetic particles); but studies showed that the hazardous interaction can take place on the ground too.

In this work we compiled a complete catalogue of HSSWSs for the last solar cycle 23, from May 1996 to December 2008. The catalogue is based on previous works of [Mavromichalaki et al., 1988, 1997] with some extra features for the 23rd Solar Cycle. In this catalogue, the HSSWSs were distinguished in four different categories and an attempt was made to examine the distributions of HSSWSs with several parameters, such as the total annual number of HSSWSs, their sources and the duration of them.

1. DATA SELECTION AND ANALYSIS

For this work solar and interplanetary data obtained from the OMNI database (http://omniweb.gsfc.nasa.gov/ow.html) were used. The following parameters as the Bartels Rotation Number, the Solar Wind Flow Speed, the Solar Wind Proton Temperature, the Solar Wind Magnetic Field Magnitude and the Solar Wind Proton Density for the time period from May 1996 until December 2008 were taken into account. The IMF data were gathered from the National Space Science Data Center database (http://omniweb.gsfc.nasa.gov/html/polarity /polarity.html).

The examined time period is from May 1996 until December 2008 and covers the solar cycle 23 according to the Mashall Space Flight Center database (http://solarscience.msfc. nasa.gov). This period was divided 23 into four phases based on the solar activity that are:

1) ascending phase, from May 1996 until April 1999,
2) maximum phase, from May 1999 until December 2002,

Table 1. An example of the catalogue of the HSSWSs during the year 1996 is presented. The first column shows the number of the HSSWS (the asterisk denotes an Interrupted HSSWS). The second column shows the exact hour that the HSSWS started. The third column shows the Bartel Rotation Number and Day for that date. The fourth column shows the IMF Polarity during the HSSWS. The fifth column shows the date of maximum solar wind speed. The sixth column shows the mean solar wind speed, while the seventh column shows the maximum speed of the HSSWS. The eighth column shows the HSSWS duration. The ninth column denotes the HSSWS category (S is for Simple HSSWS, M is for HSSWS with Multiple peaks and D is for HSSWS with Data Gaps) and the tenth column shows the source of the HSSWS (CH is a stream coming from a Coronal Hole, F is a Flare generated stream, CME is a HSSWS coming from a CME and the question mark denotes that a source for that HSSWS could not be found

N	DD/MM/YYYY hh:mm	Bartel Rotation No Day	IMF Polarity	Date of maximum	V_0 [km/s]	V_{max} [km/s]	Duration [days]	Category	Source
1	12/5/1996 14:00	2223 01	+ / –	13/5/1996 21:00	326	508	2.54	S	CH
2	15/5/1996 04:00	2223 04	– / +	15/5/1996 11:00	427	511	3.42	S	CH
3	18/5/1996 14:00	2223 07	+ / –	20/5/1996 20:00	308	481	5.46	S	CH
4	24/5/1996 01:00	2223 13	+ / – / +	25/5/1996 00:00	368	469	3.96	S	?
5	28/5/1996 22:00	2223 17	+ / –	30/5/1996 00:00	344	465	4.75	S	?
6	5/6/1996 15:00	2223 25	+	6/6/1996 11:00	312	472	6.75	S	CH
7	15/6/1996 20:00	2224 08	–	16/6/1996 08:00	332	428	3.04	S	CH
8	18/6/1996 22:00	2224 11	+	19/6/1996 08:00	384	526	4	S	CH
9	2/7/1996 12:00	2224 25	+	4/7/1996 03:00	341	554	8.25	S	CH
10	11/7/1996 19:00	2225 07	+ / –	13/7/1996 09:00	310	416	4.29	D	F
11	21/7/1996 07:00	2225 17	+	22/7/1996 00:00	364	490	3.42	D	CH
12	28/7/1996 12:00	2225 24	+	1/8/1996 06:00	307	556	9.63	M	CH
*13	14/8/1996 09:00	2226 14	+	14/8/1996 21:00	361	510	1.92	S	CH
14	16/8/1996 08:00	2226 16	+	17/8/1996 08:00	406	584	6.04	S	CH
15	28/8/1996 15:00	2227 01	+	29/8/1996 23:00	385	626	6.33	M	CH
16	4/9/1996 00:00	2227 08	–	6/9/1996 15:00	315	444	5.79	S	?

3) descending phase, from January 2003 until December 2006,
4) minimum phase, from January 2007 until December 2008.

Using the criteria presented above, the HSSWSs over the solar cycle 23 were determined and a total number of 710 HSSWSs were well defined. A catalogue with all these HSSWSs and their parameters was compiled. An example of this catalogue is presented in Table 1. The first column shows the number of the HSSWS (the asterisk denotes an Interrupted HSSWS). The second column shows the exact hour that the HSSWS started. The third column shows the Bartel Rotation Number and Day for that date. The fourth column shows the IMF Polarity during the HSSWS. The fifth column shows the date of maximum solar wind speed. The sixth column shows the mean solar wind speed, while the seventh column shows the maximum speed of the HSSWS. The eighth column shows the HSSWS duration. The ninth column denotes the HSSWS category (S is for Simple HSSWS, M is for HSSWS with Multiple peaks and D is for HSSWS with Data Gaps) and the tenth column shows the source of the HSSWS (CH is a stream coming from a Coronal Hole, F is a Flare generated stream, CME is a HSSWS coming from a CME and the question mark denotes that a source for that HSSWS could not be found.

The distribution of the total number as well as of the different categories of the HSSWSs during the phases of solar cycle 23 is given in Table 2. The second column, named Simple (S), denotes the number of the Simple HSSWSs. The third, named Multiple Peaks denotes the number of the HSSWSs with Multiple peaks. The fourth, named Data Gap denotes the number of the HSSWSs with Data Gap. The fifth, named Multiple Peaks & Data Gaps denotes the number of the HSSWSs with Multiple Peaks and Data Gap. The last column, named Consecutive to Total, denotes the ratio of the consecutive cases of HSSWSs to the total number of HSSWSs.

Table 2. A consolidated list of the number of HSSWSs in each category during the phases of solar cycle 23 is presented. Also, in this table are presented the ratio of the consecutive cases to the total number of HSSWSs for each phase of solar cycle 23

Phases of solar cycle 23	Total HSSWSs (Tot.)	Simple (S)	Multiple Peaks (M)	Data Gap (D)	Multiple Peaks and Data Gaps (D and M)	Consecutive cases of HSSWSs (C)	Ratio Consecutive Cases to Total HSSWSs (C / Tot.)
Ascending Phase	153	87	53	12	1	52	0.34
Maximum Phase	214	60	150	3	1	151	0.71
Descending Phase	239	75	157	2	5	162	0.68
Minimum Phase	104	75	29	0	0	29	0.28

The greatest ratio of Consecutive Cases to the Total number of HSSWSs appears in the maximum phase of solar cycle 23 (151 out of 214 — 71 %) followed closely by the ratio of the descending phase (162 out of 239 — 68 %). This shows that in both maximum and descending phases, the HSSWSs generation rate was very high (where 7 out of 10 HSSWSs were consecutive), unlike the ascending and minimum phases, where the HSSWSs generation rate was lower (almost 3 out of 10 HSSWSs were consecutive in those phases).

2. DEFINITION AND CATEGORIZATION OF THE HSSWS

As it was mentioned above, the definition for HSSWS as it was described in [Lindblad, Lundstedt, 1981,1983] was used. The features that were taken into account in order to determine a HSSWS are the duration of the ascending and descending phase of the stream, the number of peaks that appear in the maximum phase and the existence — or not — of data gaps. We should mention that a HSSWS can have more than one characterization. The categories that the HSSWSs have been characterized are the following and they are illustrated in Figure 2:

- Simple HSSWS.
  The simple HSSWS, as seen in Figure 2a, has a single peak and at least for three hours before the beginning and after the end of the HSSWS there is no other HSSWS present.
- HSSWS with Multiple Peaks:
  When a HSSWS has more than one peaks and each peak is closer than one day, regarding to the following one, then we characterize that HSSWS as a HSSWSs with multiple peaks, as seen in Figure 2b.
- HSSWS with Data Gap.
  When a data gap appears in any part of the HSSWS, then we describe that HSSWS as a HSSWS with data gap, as seen in Figure 2c. We accept the following approximations depending on where the data gap appears:

– if there is a data gap in the beginning of the HSSWS and the stream begins from a velocity greater than 400 km·s^{-1}, then we define the mean plasma velocity (V_0) for the pre-ascending phase as the first good velocity data point. Its duration also begins from that point; the mean plasma velocity (V_0) that follows the stream is set at 300...350 km·s^{-1};
– if the data gap appears at the peak of the stream and the maximum velocity (V_{max}) is not visible, then we define as V_{max} the greatest velocity of the good data that appears. Therefore, according to the definition of a HSSWS, if V_{max} is equal to or greater than 100 km·s^{-1} in a period lasting at least two days, we have a HSSWS.
– if there is a data gap in the descending phase and the plasma velocity has not reached the pre-ascending phase velocity (V_0), we define the end of the HSSWS as the last good velocity point. Therefore, according to the definition of a HSSWS, if the V_{max} is equal to or greater than 100km·s^{-1} in a period lasting at least two days, we have a HSSWS.

In addition, we wrote down the cases of consecutive HSSWSs. A case of Consecutive HSSWSs can be determined as follows.

- If a new HSSWS appears in less than three hours of the ending of a previous one, then we have a case of Consecutive HSSWSs, as seen in Figure 2d. For groups with more than two HSSWSs, we count a case of consecutive HSSWSs for every two consecutive HSSWSs, e.g. for a group of four HSSWSs, we have a case of three Consecutive HSSWSs.

Finally, the most important feature we added in this work is that we created a special category of HSSWSs, called Interrupted HSSWSs.

- Interrupted HSSWSs.

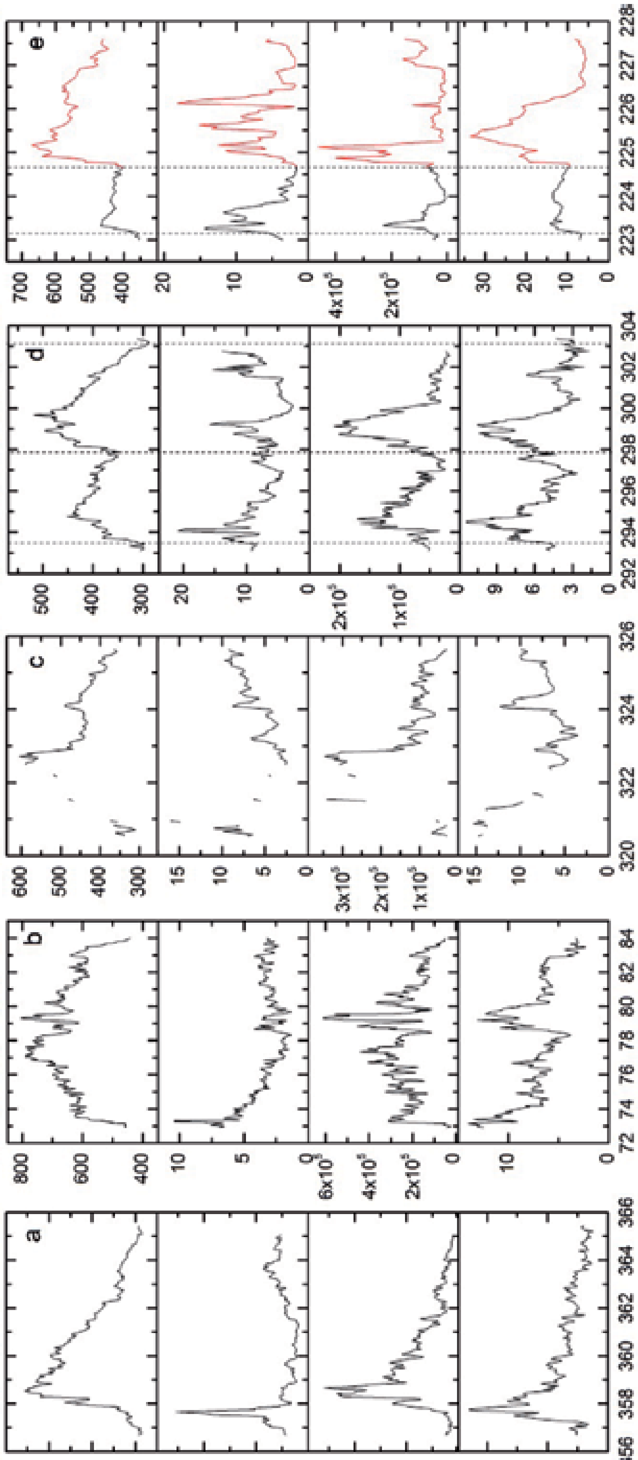

Figure 2. Categories of the HSSWS: *a* — simple HSSWS; *b* — HSSWS with Multiple Peaks; *c* — HSSWS with Data Gaps; *d* — case of Consecutive HSSWSs; *e* — interrupted HSSWS (in black)

An interruption in a HSSWSs is described as the presence of a new HSSWSs in an on-going one, as seen in Figure 2e. Based on the definition of a HSSWSs, a HSSWSs has two phases: an ascending and a descending phase. The ascending phase is defined as the period from the beginning of the HSSWSs to the moment that the HSSWSs reaches its maximum velocity. The descending phase is defined as the period of the moment that the HSSWSs has reached its maximum velocity to the end of the HSSWSs. Therefore, the interruption may take place either in the ascending phase or in the descending phase. Based on that, we categorize them into two subcategories:

– interrupted HSSWSs in the ascending phase.
These HSSWSs appear at the end of the descending phase of an ongoing HSSWS. Before the velocity of the first HSSWS reaches the pre-ascending phase mean, it raises again, due to the oncoming solar wind shock. We define that point as the preceding V_0 of the interrupted stream. Also, the V_0 that follows the HSSWS is defined as the point that the plasma velocity descends to the 330 km·s^{-1} and its duration is defined as the duration from the V_0 preceding and following the stream. Therefore, if the V_{max}, in respect to the V_0 preceding the stream, is equal to or greater than or 100 km·s^{-1} and its duration is less than 2 days, then we define the second stream as an interrupted HSSWS:
– interrupted HSSWSs in the descending phase.
These HSSWSs begin as a simple HSSWS, but the interruption occurs in its descending phase, before the plasma velocity reaches the pre-ascending phase velocity, V_0. So, the V_0 that follows the stream is defined as the point of the interruption and its duration is defined as the duration from the V_0 preceding and following the stream. Therefore, if the V_{max}, compared to the V_0 preceding the stream, is equal to or greater than or 100 km·s^{-1} and its duration is less than 2 days, then we define the stream as an interrupted HSSWS.

3. CHARACTERISTICS OF HSSWS

3.1. Total number of HSSWSs

The yearly distribution of the total number of the HSSWSs is given in Figure 3a. It is interesting that the year 2003 is the year that tended to have the most of the HSSWSs throughout the solar cycle 23, with approximately six HSSWSs per month. This year was characterized by a lot of extreme solar events, such as in October and November 2003. In addition, the most of the HSSWSs occurred during the descending phase with a percentage of 33.7 % of the total number of 710 HSSWSs during this cycle, as it is illustrated in Figure 3b. Then the ascending phase and the maximum phase follow with percentages of 21.5 % and 30.1 % respectively, while, during minimum phase, the number of HSSWS is the lowest with a percentage of only 14.6 % of the total number of HSSWSs. These results are in agreement with the results of the previous cycles 20, 21 and 22. [Maris, Maris, 2005] concluded that, during the solar cycles 20–22, the frequency of the streams was higher during the descending and minimum phases of cycles 20, 21 and 22, regardless of their solar sources (coronal holes/solar flares).

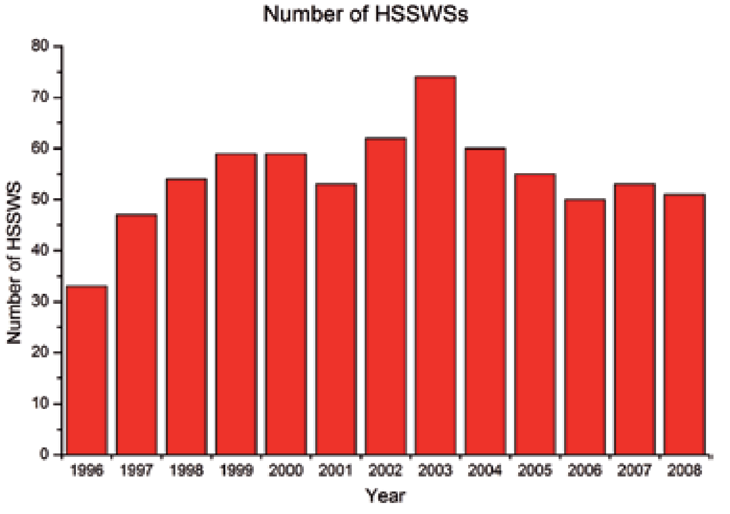

a

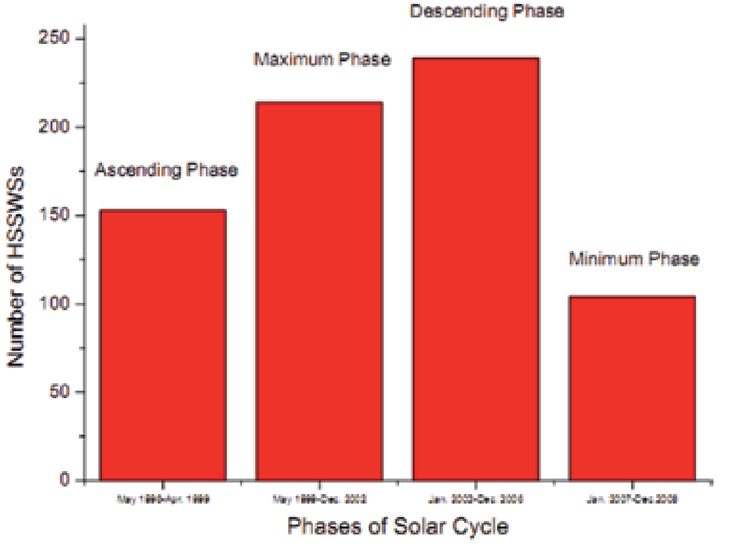

b

Figure 3. *a* — annually number of HSSWSs for solar cycle 23 (from May 1996 to December 2008); *b* — total number of HSSWSs in each phase of the solar cycle 23

3.2. Duration of HSSWSs

Previous studies of the solar cycles 20, 21 and 22 have shown that the distribution of the duration of the HSSWSs shows a maximum around 4–6 days for the even cycles and almost 6–8 days for the odd ones. The odd cycles appeared more active than the even cycles [Mavromichalaki, Vassilaki, 1998]. Also, [Gupta, 2010] divided the streams of 23rd Solar Cycle into three categories, namely: 1) short-duration High Speed Streams (HSS), those with $\Delta t \leqslant 4$ days; 2) medium-duration HSS with 4 days $< \Delta t \leqslant 8$ days; 3) long-duration HSS, those with $\Delta t \geqslant 8$ days with percentages 12, 46 and 43 % out of total 465 high-speed streams observed. Additionally, they observed that the short-duration HSS are more frequent in increasing phase, the

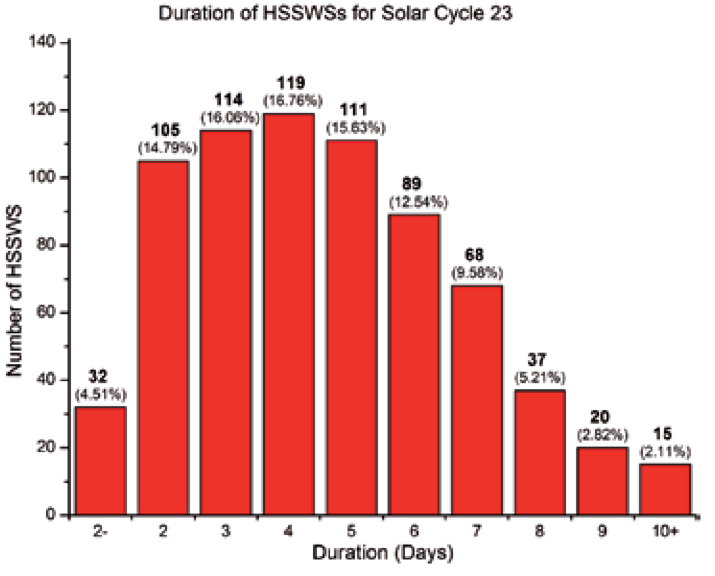

a

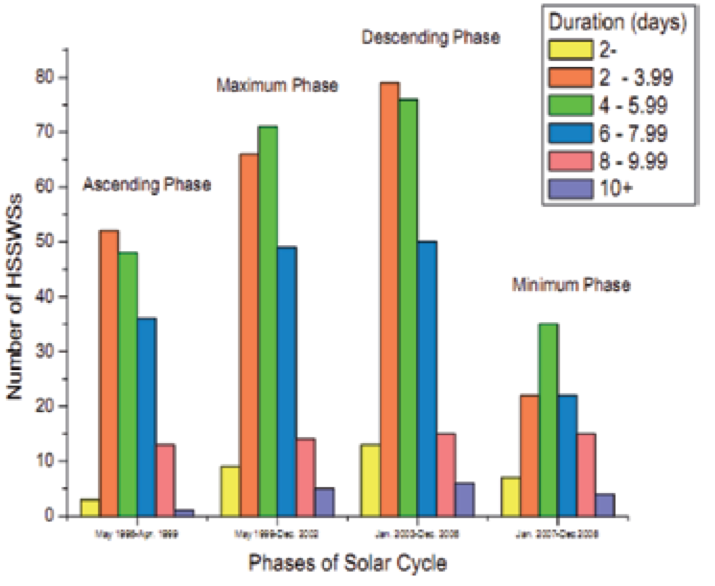

b

Figure 4. *a* — distribution of the HSSWSs duration during solar cycle 23; *b* — distribution of the HSSWSs duration during the different phases of the solar cycle 23

medium-duration HSS are less in declining phase and the last category of long-duration HSS prevail during maximum and decreasing phase of solar cycle 23.

In this study, the HSSWSs have been divided into the following bins, as seen in Figure 4a, regarding their duration:

1) HSSWSs with duration less than or equal to 1.99 days (they are symbolized as 2 days),
2) HSSWSs with duration between 2 and 3.99 days,
3) HSSWSs with duration between 4 and 5.99 days,
4) HSSWSs with duration between 6 and 7.99 days,

5) HSSWSs with duration between 8 and 9.99 days,
6) HSSWSs with duration equal to or greater than 10 days, symbolized as 10^+ days.

This division revealed that the prevalent HSSWSs are those whose duration ranges between 4 and 5.99 days with a percentage of 32.4 % out of total 710 HSSWS observed. Considering a decreasing order, the HSSWSs appear duration between 2–3.99 days and 6–7.99 days with percentages of 30.9 and 22.11 % respectively. The fewer HSSWSs are those symbolized as 2– and 10+, where they constitute only the 4.51 and 2.11 % out of total 710 HSSWS respectively. Therefore, taking in mind the statistical error for each duration bin, in our study appeared that the most HSSWSs for solar cycle 23 last from 3 to 5.99 days. This conclusion is in agreement with the previous study of [Gupta, 2010], where the prevalent HSSWS are those they characterized as medium-duration high speed stream with duration 4 days $< \Delta t \leqslant$ 8 days (46 %).

Regarding the distribution of HSSWSs duration during the phases of the solar cycle, as seen in Figure 4b, the most HSSWSs in the ascending phase last between 2 and 3.99 days (33.99 % out of the total 153 HSSWSs in the ascending phase). In the maximum phase the HSSWSs that last between 4 and 5.99 days (33.17 % of 214 HSSWS in maximum phase) are dominate. Additionally during the descending phase prevail the HSSWSs that last from 2 to 3.99 days (33.05 % of the 239 observed HSSWSs for the descending phase), followed closely by the HSSWSs that last from 4 to 5.99 days (31.80 % of the 239 observed HSSWSs). Finally, the most frequent HSSWS during the minimum phase are to be those with duration between 4 and 5.99 days (33.65 % out 104 HHSWSs during minimum). It is worth to be mentioned that the most frequent Interrupted HSSWSs (symbolized as 2-days) are observed during the descending phase with a percentage of 40.6 % of the total number of them; that's a result of the high solar activity during that phase, where HSSWSs were constantly generated, leaving no space for the interrupted HSSWSs to come up as a normal HSSWS. Also the HSSWSs characterized as 10+ days appear most frequently during the descending phase 40.0 % of the total 15 HSSWSs in the 10+ days group. Finally, it is important to be mentioned that the HSSWS with the maximum duration of 16.71 days is observed during the maximum phase.

3.3. Maximum Speed of HSSWSs

For the purposes of this distribution, the total number of 710 HSSWSs has been divided into bins of 100 km·s^{-1}, from 400 to 1199 km·s^{-1} in each of the four phases of the solar cycle 23. Also the streams with data gaps in the V_{max} have been taken into consideration. In an overview, as seen in Figure 5, taking into account the phases of the solar cycle according to this study, in the ascending phase the most HSSWSs observed to have V_{max} between 400 and 499 km·s^{-1} (almost 41.83 % of 153 HSSWS in ascending phase). In the maximum phase, V_{max} increases to 500...599 km·s^{-1} (35.05 % of 214 HSSWSs in maximum phase). Then, in the descending phase V_{max} keeps rising with a 29.29 % of the 239 descending phase HSSWSs have V_{max} between 500 and 599 km·s^{-1}, but also 32.22 % of them have V_{max} between 600...699 km·s^{-1}. Finally, in the minimum phase the most HSSWSs (41.35 % of 104 streams) have V_{max} of 600...699 km·s^{-1}.

A further analysis for the phases of solar cycle 23 shows, as already referred, in ascending phase the highest number of HSSWSs has V_{max} of 400...499 km·s^{-1}. In a decreasing order follow the 500...599 km·s^{-1} bin (35.95 %) and the 600...699 km·s^{-1} bin (16.99 %). The amount of 1.96 % of HSSWSs in the ascending phase belongs equally and respectively to the bins of 700...799 km·s^{-1} and 800...899 km·s^{-1}. Moreover, there is not any HSSWS observed with V_{max} up to 900 km·s^{-1}, while two HSSWSs have data gaps is their V_{max}.

In the maximum phase the number of HSSWSs in the bin of 400...499 km·s^{-1} is starting to decrease (28.04 % out of 214 HSSWSs) and the predominant bin is those of 500...599 km·s^{-1} (35.05 %). Considering the decreasing order follow the 600...699 km·s^{-1} bin (22.90 %), the 700...799 km·s^{-1} bin (8.88 %) and the 800...899 km·s^{-1} bin (2.80 %). It is worth to be mentioned that two HSSWSs are observed with V_{max} between 900 and 999 km·s^{-1} and two HSSWSs with V_{max} between 1000 and 1099 km·s^{-1} bin (0.93 % respectively). Also only one HSSWS has data gap at V_{max}.

Subsequently, in descending phase, the number of HSSWSs belonging to the 500...599 km·s^{-1} bin is lower than the number of HSSWSs belonging to the 600...699 km·s^{-1} bin. In this phase, only 12.55 % of the HSSWSs belong to the 400...499 km·s^{-1} bin, while the 17.15, 5.86 and 1.67 % of the 239 descending phase HSSWSs constitute the 700...799 km·s^{-1} bin, 800...899 km·s^{-1} bin and 900...999 km·s^{-1} bin respectively. Also the HSSWSs with higher V_{max} are observed more frequently, as four of the 239 HSSWSs have V_{max} between 900 and 999 km·s^{-1} and two HSSWSs have V_{max} between 1000 and 1099 km·s^{-1}. Finally, in that phase, it is observed the HSSWS with the highest V_{max} of the Cycle, reaching a speed of 1189 km·s^{-1}.

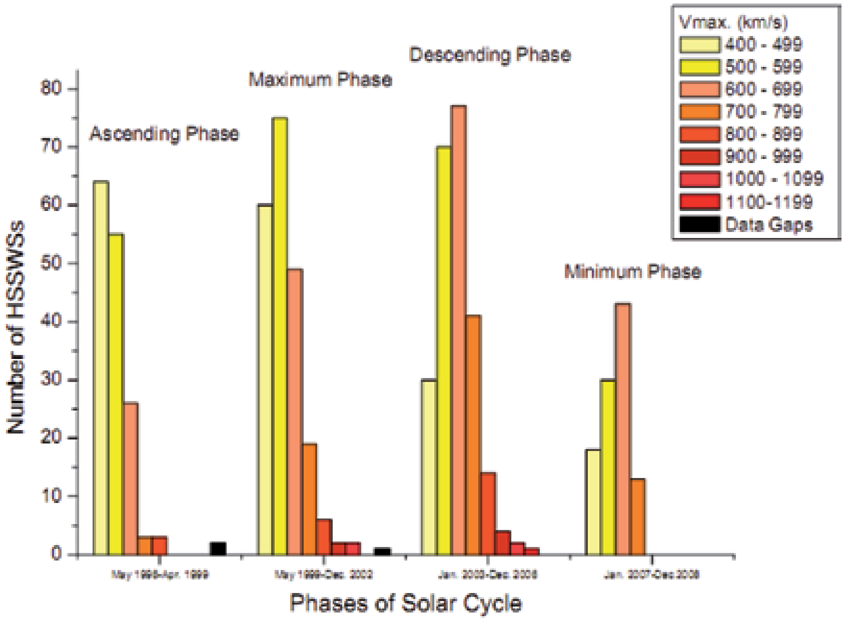

Figure 5. Distribution of the V_{max} of each HSSWS in the phases of the solar cycle 23. It is clearly notable that the peak of the V_{max} distribution is increasing through the solar cycle, until the Descending Phase and it stays at that level in the Minimum Phase (instead of dropping)

At last, as it is observed in minimum phase, most of the HSSWSs belong to the 600...699 km·s^{-1} bin, and they follow in decreasing order: 500...599 km·s^{-1} bin (28.85 %), 400...499 km·s^{-1} bin (almost 17.30 %) and 700...799 km·s^{-1} bin (12.50 %). It is worth to be mentioned that only one HSSWS has V_{max} between 800 and 899 km·s^{-1}. Finally, during the descending and minimum phase there is not any data gap at V_{max} of any HSSWS.

In conclusion, it is obvious that the V_{max} distribution peak keeps rising until the descending phase (where it reaches the values of 600...699 km·s^{-1}) and instead of dropping in the minimum, it stays at those values. In addition, it is important to mention that the highest values of observed V_{max}, considering an increasing order of V_{max}, are: 922 km·s^{-1} (in 2002), 1010 km·s^{-1} (in 2000), 1027 km·s^{-1} (in 2004), 1040 km·s^{-1} (in 2001), 1059 km·s^{-1} (in 2005) and 1189 km·s^{-1} (in 2003).

3.4. Sources of HSSWSs

As it is being mentioned, the possible sources of HSSWSs are the coronal holes and the solar flares. Therefore, the HSSWSs were classified into two categories, corotating and flare-generated streams, respectively. [Lindblad, Lundstedt, 1981, 1983; Lindblad et al., 1989] presented the HSSWSs observed by near-Earth spacecraft in the periods 1964–1975, 1975–1978 and 1978–1982 (solar cycles 20 and partly 21). [Mavromichalaki et al., 1988] presented a catalogue of HSSWSs for the period 1972–1984 and, as a continuation of the previously published catalogue, [Mavromichalaki, Vassilaki, 1998] presented the HSSWSs catalogue for the period 1985–1996 (cycle 22) and they classified them into the above mentioned categories. The conclusions of the last paper indicates that the number of flare-generated streams is greater around the solar maximum (1969, 1979 and 1989 of cycles 20, 21 and 22 respectively), while corotating streams are more around the solar minimum. Also, [Maris, Maris, 2005] followed this classification of HSSWSs for the solar cycles 20–22: the ones produced by coronal holes (CH_HSPS) and the ones produced by solar flares (FG_HSPS). They revealed that the CH_HSPS prevail during the minimum phases of solar cycles, due to the large extended coronal holes towards the equator registered in the minimum phases of solar cycles, while the FG_HSPS variation follows the 11-year cycle of sunspots.

Furthermore, [Mavromichalaki, Vassilaki, 1998] concluded that the activity of solar cycle 21, which is an odd cycle, was greater than the activity of 20th and 22nd solar cycles, which are even cycles. This fact shows a periodicity, due to the 22-year variation of solar magnetic field [Legrand, Simon, 1981; Simon, Legrand, 1992; Mavromichalaki et al., 1997; Mavromichalaki, Vassilaki, 1998]. Also this indicates different behaviors between odd and even cycles, such as the large number of flare-generated streams during the odd cycles and the appearance of two maxima during the even cycles. [Maris, Maris, 2005] showed that the solar cycles 20 and 22 have similar dynamics of FG_HSPS and CH_HSPS parameters during maximum, descending and reversal intervals. They revealed that the solar cycle 21 dominance of all the CH_HSPS parameters against the 20th and 22nd solar cycle, during almost all phases, could be due to the same structure of Hale cycle, though solar cycle 21 has a larger number of FG_HSPS as the even cycles.

In addition to our study, it is worth to be mentioned that the corotating streams are connected with simple decreases of cosmic rays recorded at ground based station and the flare-generated streams produce Forbush decreases on Earth [Iucci et al., 1979; Mavromichalaki et al., 1988]. Also strong flares recorded by Neutron Monitors on Earth, reveal large level enhancements (GLE) associated with energetic solar proton events, such as those of 22nd solar cycle [Belov, Eroshenko, 1996].

In an earlier paper [Gupta, 2010], divide the HSSWSs of solar cycle 23 into five groups, namely associated with: 1) a single coronal hole (SCH); 2) a single mass ejection (SME); 3) multiple coronal holes (MCH); 4) multiple mass ejections (MME); 5) compound streams associated with both coronal hole(s) and mass ejection(s) (CMP). They concluded that out of 465 streams the majority of them (43 %) produced by a single coronal hole, and in a descending order follow: the compound streams (26 %), the streams produced by multiple coronal holes (18 %), a single mass ejection (9 %) and the minority of them (4 %) are related to multiple mass ejections.

In this work, as a continuation of the previous works of [Mavromichalaki et al., 1988; Mavromichalaki, Vassilaki, 1998], the HSSWSs are considered as follows: corotating streams (CH) which are those that are emitted by coronal holes and flare-generated streams (F) which are those that are associated with active regions of Sun emitting solar flares. Also, for this Solar Cycle, because of the availability of good quality coronogragh data, an attempt is made to take in mind the CMEs, as a possible source of HSSWSs. Therefore, the 710 HSSWSs are divided into six groups:

1) corotating streams, those that are produced by corotating coronal holes; marked with the symbol CH;
2) flare-generated and CME-generated streams, those that are produced by both flare and CME; marked with the symbol F/CME;
3) flare-generated streams, those that are produced only by a flare; marked with the symbol F;
4) CME-generated streams, those that are produced by only a CME; marked with the symbol CME;
5) flare-generated and CME-generated streams in the case that the possible active origin is not clear; marked with the symbol F/CME ?
6) those that their origin is not clear; marked with the symbol: ?

In these terms we have statistically studied the distribution of HSSWS per year and phase of solar cycle.

The annually distribution of HSSWSs on the basis of their origin, as shown in Figure 6a, reveals that the most streams of solar cycle 23 are corotating streams (CH). The majority of CH HSSWSs (56 CH) is produced in 2003 and the minority of them (21 CH) in 2001, while the majority of streams that are related to both flares and CMEs (11 F/CME) were observed in 2001. As shown the maximum of the distribution of flare-generated streams (29 F) is placed in the year 2000. It is worth to be mentioned that we had individual CME-generated streams (CME) that give no notable distribution to show an 11-year variation. Those individual CME HSSWS take place in years 1997 and 2008. The same fact is observed for the flare-generated and CME-generated streams in the case that the possible active origin is not clear (F/CME ?), where individual cases take place in the years 1999, 2000, 2001, 2002, 2003, 2004 and 2006. Also a number of ten HSSWSs have doubtful and no clear origin (?). Their number in comparison to the total number of HSSWSs presents a negligible error.

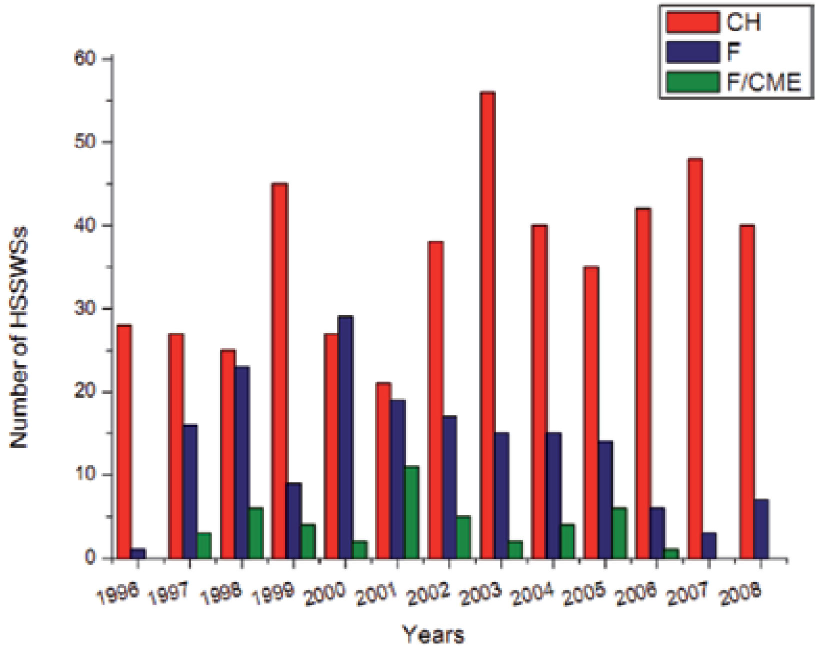

a

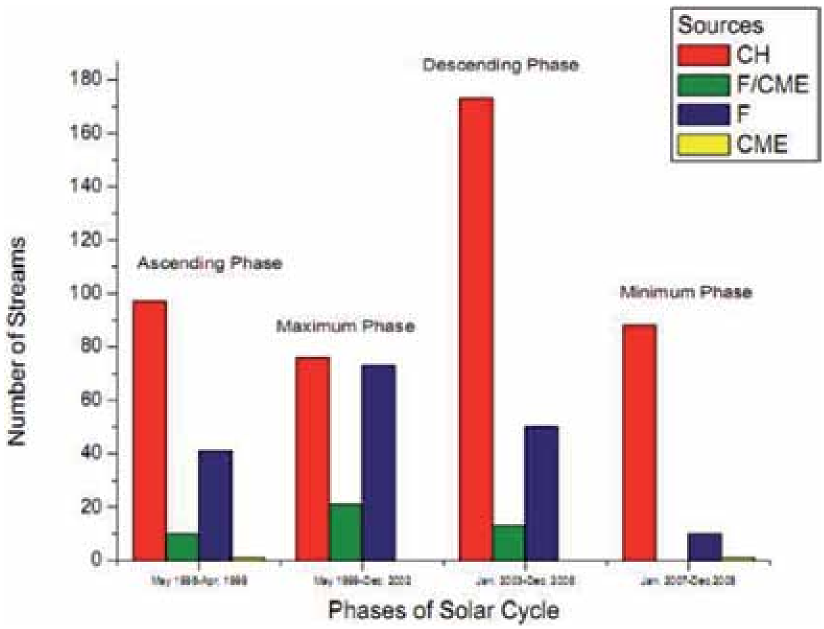

b

Figure 6. *a* — annual distribution of the sources of the HSSWSs6; *b* — distribution of the sources of the HSSWSs for each phase of solar cycle 23

Regarding the source distribution via the mentioned phases of solar cycle 23, as presented in Figure 6b, it is proved that the most HSSWSs are CH and take place in the descending and the ascending phases of cycle, where 131 CH (39.9 % of total 434 CH) and 97 CH (22.4 %) are shown respectively. On the other hand the F and the F/CME HSSWSs show an 11-year variation. Most of them, in percentages of 42 % of total 174 F and 47.7 % of 44 F/CME HSSWS, are observed in maximum phase, but still the number of them is significantly lower than the CH HSSWSs. Finally, for consistency, the two individual CME HSSWSs are considered and they are observed in ascending and minimum phase, but this result is not significant, due to its few data.

Concluding, the majority of HSSWSs are CH HSSWSs, despite the fact that the solar cycle 23 is an odd cycle. This is shown in both Figures 6a and b, where 63.4 % out of total 153 HSSWSs in ascending phase, 35.5 % of 214 HSSWSs in maximum, 72.4 % of 239 HSSWSs in descending phase and 84.6 % of 104 HSSWSs during minimum are CH HSSWSs. [Maris, Maris, 2005] come, also, in that conclusion, where it is mentioned that "the best-established sources of the HSPSs are the coronal holes- the regions with open magnetic fields". The majority of F HSSWSs appeared in maximum phase (34.1 % of 214 HSSWS) is in agreement with previous studies, where the same was observed in maximum phase (1969, 1979, 1989 for solar cycles 20, 21 and 22 respectively), as a result to the fact that the large coronal holes existing during the solar minimum giving a lot of corotating streams. As a total conclusion, the number of F and F/CME HSSWSs is higher around the maximum phase showing an 11-year variation; this is in agreement with what was observed by plotting the number of F HSSWSs for each year for the solar cycles 20–22 [Mavromichalaki, Vassilaki, 1998] and the statistical study of flare-generated streams of the period 1964–1996 [Maris, Maris, 2005]. In contrast, the CH HSSWSs number is high throughout the solar cycle, but according to [Mavromichalaki, Vassilaki, 1998] it was expected to be high only in the ascending phase and in the minimum.

CONCLUSIONS

A detailed analysis of the HSWSs registered in the time interval 1966–2008 covering the solar cycle 23, was carried out and a great number of 710 HSSWSs were well defined. It is noted that 434 of them were generated by corotating coronal holes (CH), 261 were generated by flares, CMEs or both (F, CME or F/CME) and the origin of 15 was not clear. It means that more than half of them are generated by coronal holes, fact that it was not appeared in previous cycles.

It is known that the last solar cycle 23 was one of the most active cycles characterized by many extreme solar events. In this study it was observed that the maximum appearance of HSSWSs (73 HSSWSs) took place in the year 2003 that is in the descending phase of this cycle, right after the secondary maximum of the solar activity. In addition, the greatest ratio of consecutive HSSWSs appears in both the maximum and descending phases of solar cycle 23, where 7 out of 10 HSSWSs were consecutive.

The average duration of the HSSWSs of the solar cycle 23 through our work is 3 to 5 days. Compared to our previous works [Mavromichalaki et al., 1988; Mavromichalaki, Vassilaki, 1998], we observed that the duration of the HSSWSs tends to drop with every solar cycle: the average duration of the 21st solar cycle HSSWSs was 6...7 days, the one of the 22nd solar cycle was 4–5 days and as we mentioned before, the one of the 23rd solar cycle was 3–5 days. This might be a hint of a more active Sun as the cycles go by, because the continuous generation of HSSWSs prevents the Sun of generating long HSSWSs. Also, for this cycle, we can accept the fact that we had more advanced equipment and more spaceships for the detection of the solar wind characteristics. In addition, we had the opportunity of analyzing a complete data base with data from all the spaceships and that makes the work for the 23^{rd} solar cycle more reliable than the work of previous cycles.

As concerns the maximum velocity of the HSSWSs we concluded that in the ascending solar phase most of the HSSWSs observed to have V_{max} between 400 and 499 km·s^{-1}, in the maximum phase the peak of V_{max} distribution increases to 500...599 km·s^{-1}, in the descending phase the V_{max} peak keeps rising as most of the HSSWSs occurred have a V_{max} of 500...599 km·s^{-1} and 600...699 km·s^{-1} and in the minimum phase dominates a V_{max} of 600...699 km·s^{-1}. It is notable that the HSSWSs with the highest values of V_{max} (900...999, 1000...1099 and 1100...1199 km·s^{-1} bins) are observed more frequently in the maximum and the descending phases. In time evolution it is clear that V_{max} peak increases until descending phase, where it stays stable to the minimum phase; though in the minimum phase V_{max} higher than 800 km·s^{-1} vanished.

Finally, the annually HSSWSs source distribution showed that the most HSSWSs that occurred in solar cycle 23 are CH HSSWSs, with the maximum of their distribution shown in the year 2003 and the minimum in the year 2001. The majority of F/CME and F HSSWSs combined occurred in 2001, 2000 and 1998 respectively. The CME and F/CME ? HSSWSs give no notable distribution due to their few data points, while 10 HSSWSs are found with doubtful origin. Although that solar cycle 23 is an odd one, the distributions of HSSWSs according to their sources during the considered phases, reveal that most of the CH HSSWSs occurred during the descending and ascending phases, but in general there were many CH HSSWSs through the whole cycle. Also, most of the F and F/CME HSSWSs are observed in the maximum phase, showing an 11-year variation. The conclusions of this work are in good agreement with the studies of the solar cycles 20, 21 and 22.

In summary, we can say that one of the most dynamical interplanetary phenomena of Solar-Terrestrial Physics is definitely the passage of solar wind streams near the Earth environment. Studies of various aspects of the solar wind velocity variability with time in the ecliptic plane revealed a solar wind tendency to be organised as stream structures e.g. [Iucci et al., 1979; Lindblad, Ludstedt, 1981]. In particular, the characteristics and the long-term variations in the occurrence rate of high-speed streams for solar cycles 20, 21 and 22 have been studied in [Mavromichalaki, Vassilaki, 1998; Maris, Maris, 2005]. Reference catalogues of high-speed solar wind streams observed near the Earth have been produced, considering two possible solar sources, coronal holes and active regions emitting solar flares. In this work a new high speed streams source concerning the CMEs is added, as CMEs data are now available. In the future an extended study concerning the sources of this great number of these events during the solar cycle 23 will be very useful for Space Weather studies.

Acknowledgments. Thanks are due to all colleagues that are working and provide kindly all this amount of solar and interplanetary data used in this work. Acknowledgment is also held to the Special Research Account of the National and Kapodistrian University of Athens, for supporting G. Xystouris to present this work in the Space Weather Effects on Humans Conference held in Moscow (3–7 June 2012).

REFERENCES

[Bame et al., 1976] *Bame S.J., Asbridge J.R., Feldman W.C., Gosling J.T.* Solar cycle evolution of high-speed solar wind streams // Astrophysics J. 1976. V. 207. P. 977–980.

[Belov et al., 1996] *Belov A.V., Eroshenko E.A.* Proton spectra of the four remarkable GLE in the 22nd solar cycle // Radiation Measurements. 1996. V. 26. N. 3. P. 461–466.

[Broussard et al., 1978] *Broussard R.M., Tousey R., Underwood J.H., Sheeley N.R. Jr.* A survey of coronal holes and their solar wind associations throughout sunspot cycle 20 // Solar Physics. 1978. V. 56. P. 161–183.

[Gosling et al., 1976] *Gosling J.T., Asbridge J.R., Bame S.J., Feldman W.*C. Solar wind speed variations — 1962–1974 // J. Geophysical Research. 1976. V. 81. P. 5061–5070.

[Gupta, 2010] *Gupta V., Badruddin.* High-Speed Solar Wind Streams during 1996–2007: Sources, Statistical Distribution, and Plasma/Field Properties // Solar Physics. 2010. V. 264. P. 165–188.

[Hollweg, 1974] *Hollweg J.V.* Hydromagnetic waves in interplanetary space // Publications of the Astronomical Society of the Pacific. 1974. V. 86. P. 561–594.

[Intriligator, 1977] *Intriligator D.S.* Evidence for a constant speed of shock propagation between 0.8 AU and 2.2 AU // Proc. 15th Intern. Cosmic Ray Conf. (ICRC). 1977. V. 11. P. 225–229.

[Iucci et al., 1979] *Iucci N., Parisi M., Storini M., Villoresi G.* High-speed solar-wind streams and galactic cosmic-ray modulation // Nuovo Cimento C Geophysics Space Physics. 1979. V. 2. P. 421–438.

[Legrand, Simon, 1981] *Legrand J.P., Simon P.*A. Ten cycles of solar and geomagnetic activity // Solar Physics. 1981. V. 70. P. 173–195.

[Lindblad, Lundstedt, 1981] *Lindblad A., Lundstedt H.* A catalogue of high-speed plasma streams in the solar wind // Solar Physics. 1981. V. 74. P. 197–206.

[Lindblad, Lundstedt, 1983] *Lindblad B.A., Lundstedt H.* A catalogue of high-speed plasma streams in the solar wind 1975–1978 // Solar Physics. 1983. V. 88. P. 377–382.

[Lindblad et al., 1989] *Lindblad B.A., Lundstedt H., Larsson B.* A third catalogue of high-speed plasma streams in the solar wind — Data for 1978–1982 // Solar Physics. 1989. V. 120. N. 1. V. 145–152.

[Maris, Maris, 2005] *Maris O., Maris G.* Specific features of the high-speed plasma stream cycles // Advances in Space Research. 2005. V. 35. P. 2129–2140.

[Mavromichalaki, Vassilaki. 1998] *Mavromichalaki H., Vassilaki A.* Fast Plasma Streams Recorded Near the Earth During 1985–1996 // Solar Physics. 1998. V. 183. P. 181–200.

[Mavromichalaki et al., 1988] *Mavromichalaki H., Vassilaki A., Marmatsouri E.* A catalogue of high-speed solar-wind streams — Further evidence of their relationship to Ap index // Solar Physics. 1988. V. 115. P. 345–365.

[Mavromichalaki et al., 1997] *Mavromichalaki H., Vassilaki A., Tsagouri I.* Features of the high-speed plasma streams during the last solar cycle // Joint European and National Astronomy Meeting (JENAM-97): Abstr. 1997. P. 83.

[Morley, 2009] *Morley S.K., Rouillard A.P., Freeman M.P.* Recurrent substorm activity during the passage of a corotating interaction region // J. Atmospheric and Solar-Terrestrial Physics. 2009. V. 71 P. 1073–1081.

[Parker, 1959] *Parker E.* Extension of the Solar Corona into Interplanetary Space // J. Geophysical Research. 1959. V. 64. P. 1675–1681.

[Simon, Legrand, 1992] *Simon P.A., Legrand J.P.* Toward a model of a two-component solar cycle // Solar Physics. 1992. V. 141. N. 2. P. 391–410.